Water-Assisting Proton Transfer Isomerization of the HNO/HON System in the Singlet State: On the Number of the Effective Water Molecules

Zhiqiang Li,[†] Yuxiang Bu,*[,†,‡] and Hongqi Ai[†]

Institute of Theoretical Chemistry, Shandong University, Jinan, 250100, P.R. China, and School of Chemistry, Qufu Normal University, Qufu, 273165, P.R. China

Received: January 26, 2004; In Final Form: June 1, 2004

A density function theory study is presented for the HNO ⇌ HON isomerization assisted by *m* water molecules ($m = 1-4$) on the singlet state potential energy surface. Two modes are considered to model the catalytic effect of *m* water molecules: (1) water molecule(s) directly participate in forming a proton transfer loop with HNO/HON species and (2) water molecules are out-of-loop, modeling the outer-sphere water effect from the other water molecules directly H-bonded to the loop (referred to as out-of-loop waters). Two mechanisms are proposed for the mono-water-assisting isomerizations and one for each of the other cases. The reactant and product of all groups have been characterized for all potential energy surfaces. For the monohydration mechanism, the reactant complex is connected to the product complex via two determined saddle points, and the reaction heat is 35.5 kcal·mol^{-1} at the B3PW91/6-311++G** level. The corresponding forward/backward barrier lowerings are obtained as 7.4/1.2 (AT2) and 34.1/28.3 (AT1) kcal·mol^{-1}, respectively, compared with the no-water-assisting isomerization barrier T (72.6/31.3 kcal·mol^{-1}). When one to three out-of-loop water molecules are considered, their effects on the three energies are small, and the deviations are not more than 2 kcal·mol^{-1} compared with the original monohydration assisting case (AT1). For the dihydration assisting mechanism, the reaction heat is 30.5 kcal·mol^{-1}, and the forward/backward barrier lowerings become 41.7/30.9 kcal·mol^{-1} compared to T. Further increasing by 1−2 out-of-loop waters does not obviously change the energetics. For trihydration, the forward/backward barriers further decrease as 43.5/30.9kcal·mol^{-1}, and the reaction heat decreases by 12.4 kcal·mol^{-1}. The same is true for the influence of the additional out-of-loop waters. However, when four water molecules are involved in the reactant loop, the corresponding energy aspect increases slightly. The forward/backward barrier lowerings for the tetrahydration mechanism become 41.8/29.4 kcal·mol^{-1}, respectively, smaller by 1.7 and 1.5 kcal·mol^{-1} than the trihydration situation. Therefore, it can be concluded that the most favorable hydration-assisting mode should be one with three in-loop waters. Such hydration-assisting isomerization pathways can exist in water-dominated environments, for example, in the organism, and are significant to energy transferring.

1. Introduction

That the nitric oxide (NO) can be biosynthesized in mammalian cells has brought intense interest in the physiological chemistry of nitrogen oxides (NO), and there is diverse biological activity associated with NO and NO^- derived species.[1] By contrast, the reduced congeners such as nitroxyl (HNO) and its conjugate base (NO^-) are less well understood, and consequently their role in biology is not clear. The importance of HNO or NO^- in biology has often been neglected or dismissed, in part because NO metabolism is thought to be primarily oxidative in nature, and because HNO is thought to be only metastable,[2] a strong acid,[3] and to dimerize readily.[4] The nitroxyl (HNO) is known to be able to be formed under physiological conditions; for example, oxidation of *N*-hydroxy-L-arginine (an intermediate in NO biosynthesis)[5] may generate HNO. Recent works also demonstrated that *S*-nitrosothiols playing a key role in a variety of physiological processes can react with thiols to generate HNO and further serve as a possible source of nitrosonim (NO^+) or nitroxyl (NO^-) ions,[6] and the generation of a catalytic antibody may release nitroxyl that is further oxidized to nitric oxide (NO) in the presence of superoxide dismutase.[7,8] Nitroxyl (HNO) has been found to have much biological activity, such as, it can act as a potent cytotoxic agent that causes double-stranded breaks in DNA, depletion of cellular glutathione,[9] as well as elicitation of smooth muscle relaxation.[10] Similarly, for the HON (the isomer of HNO), although it has been evidenced to exist both theoretically and experimentally,[11] it is not generally known that whether the HON is a participant in the physiological chemistry of HNO.[12] All these possibilities have engendered a rapidly growing interest in the biological roles of nitroxyl, and a number of research groups have been recently involved in the related studies mainly for slow release of nitroxyl into various environments.[13−19] In addition, some prodrug release systems are also of particular biological significance since nitric oxide acts as a chemical messenger for a number of fundamental bioregulatory processes, including blood pressure regulation and memory.[20−22] Originally, NO was identified in biological systems as the active principle of EDRF (endothelium-derived relaxing factor).[23] The biological effect of nitric oxide can be mimicked by NO-releasing drugs such as nitroglycerine, which are commonly used to treat angina and hypertension.

On the other hand, the HNO and its derivatives are also very important in atmospheric chemistry. They may take part in some

[†] Shandong University.
[‡] Qufu Normal University.

10.1021/jp049636t CCC: $27.50
Published on Web 07/02/2004

fundamental processes such as pollution formation, energy release in propellants, and fuel combustion.[24,25] Therefore, the mechanistic interpretations of observed effects require a detailed knowledge of the underlying chemistry of nitroxyl and the species derived from it.

In view of the importance of HNO and its derivatives in biological systems and atmosphere chemistry, many works have focused on the exploration of the character of their electronic states and various structural properties.[11,26−39] HNO was experimentally recognized early,[34] and theoretical progresses of interest have also been made. Yet, according to the results of some theoretical studies the existence of nitroxyl (HON, also isonitroso hydrogen) besides HNO has been anticipated, but until recently it was not experimentally evidenced.[11] Gas-phase investigations indicate that these species (HNO or HON) possess not only complicated dissociation channels, but also a complicated isomerization mechanism.[33] Although a large amount of experimental and theoretical data are available for HNO and HON in the gas phase up to now, our understanding of their photochemistry remains far from complete. Further, the studies closely relevant to their biological processes are absent. In particular for the proton-transfer isomerization between them, HNO ⇌ HON, besides their various dissociation channels, all those investigations were limited to the gas phase although they have provided much valuable information.[11,32,33,35−39] From those investigations three important aspects should be noted: (i) There exists a large isomerization barrier greater than the dissociation threshold on both the ground state and the low-lying singlet excited state potential energy surfaces (PES). In contrast, only a small isomerization barrier exists on the low-lying triplet excited state PES. This provides support for the nitrogen cycle, which relies on interconversion between HON and HNO isomers not only on the ground-state PES but also on the excited-state PESs.[33] (ii) The isomerization reaction is spin-forbidden if it is to connect the ground states of HON ($^3A''$) and HNO ($^1A'$).[30,39] (iii) There may be a photochemical equilibrium between HNO and HON, which is presumably reached by the dissociation of the two isomers into NO radicals and H atoms[11] and then recombinations.

How about the situation regarding them in solution, in actual biological systems? How about the medium effect on the dissociations and isomerizations regarding them? Obviously, this aspect is far less availabile than that on the gas phase.

Since water is also an abundant species in the organism and the atmosphere, it can be predicted that the considerable coupling interaction of either HNO or HON with water molecules may significantly influence their stability and the isomerization mechanism. Unfortunately, to our best knowledge, no investigations of this kind have been reported up to now. Therefore, it is of interest to explore the role of the water in catalyzing this isomerization reaction. The aim of this paper is to couple explicit water molecules with HNO or HON to model the possible isomerization processes and to explore the actual HNO−HON interconversion mechanism and the optimal interconversion pathway including the most effective number of explicit water molecules for improving the interconversion. This clue regarding the explicit water assisting model is also motivated by the fact that since only some limited water molecules could enter the proximity of NO-biosynthesizing proteins or the HNO generation center, it is possible and also reasonable for a limited number of explicit water molecules to interact the HNO/HON for catalyzing the interconversion or dissociation mechanism. Of course, some side chains of amino acids may also play some roles in these interconversions. But, just the water-assisting role will be considered in this work and the later will be reported further elsewhere.

This paper is structured as follows: the computational methods that are used are presented in section 2. Section 3 presents the results of our proposed mechanisms for the monohydrated, dihydrated, trihydrated, and tetrahydrated reactions, and the comparison between all of the different pathways is also made. Finally, our conclusion is given in section 4.

2. Computational Details

The full geometrical optimizations on the HNO/HON and their different degrees of hydrated complexes have been made with use of three DFT methods with a 6-311++G** basis set, which have been demonstrated to be effective methods for yielding sufficiently accurate structure and relative energy parameters.[40−42] The three density functional methods used are B3LYP, B3P86, and B3PW91, as implemented in GAUSSIAN 98.[43] These three models combined the Becke three-parameter hybrid functional, which is a linear combination of Hartree−Fock exchange, Slater exchange, and B88 Gradient-corrected exchange,[44] with the correlation functional of Lee et al.[45] and Vosko et al.,[46] Perdew (P86),[47,48] and Perdew and Wang (PW91),[49] respectively. To confirm the energy quantities, the CCSD(t,full) single-point calculations are also performed with the 6-311++G** basis set at the B3PW91/6-311++G** geometries only for the unhydrated and monohydrated systems. For all energy quantities, the zero-point energy corrections are considered.

In calculations regarding water-assisting isomerizations, 1−4 water molecules are included to assist the proton-transfer isomerizations via two schemes: (1) 1−4 water molecules are looped with HNO/HON; (2) 1−3 water molecules are attached to the looped waters to model the outer-sphere solvent effect from the other waters directly H-bonded to the looped waters. But the total number of water molecules considered here is one, two, three, or four, respectively, forming four different hydration-assisting schemes.

Since the role of water molecules in the reactant loop is larger than that in the out-of-loop waters for the assisting, the unhydration, moohydration, dihydration, trihydration, and tetrahydration assisting modes are defined only according to the number of waters in the loop.

3. Results and Discussion

3.1. Structural Properties and Proton-Transfer Isomerization of HNO/HON. Before starting to discuss the water-assisting effect on the proton transfer isomerization of the HNO/HON system, it is very necessary to first investigate their structure properties and the fundamental character. Due to the importance in combustion, atmospheric chemistry, and biological areas, the structural property investigations of HNO/HON have continuously been the subject of theoretical and experimental works.[11,29−39] After HNO was first experimentally evidenced by Dalby,[34] many theoretical and experimental investigations have confirmed its existence, including its isomer (HON).[11] The electronic states, the spectroscopy, and the PES character have been extensively explored by different groups.[33,39] At the CCSD(T)/cc-pVQZ level, Lee and Dateo calculated the heat of formation for HNO as 26.0 ± 0.8 kcal·mol^{-1}, from which the H−NO bond energy was extracted to be 47.7 kcal·mol^{-1} (at 298 K).[29] Another important energy quantity, the proton dissociation energy, was experimentally determined to be 354.70 ± 0.40 kcal·mol^{-1} for the HNO → H^+ + NO^- dissociation.[51] In particular, the HNO ⇌ HON isomerization

TABLE 1: Structural Parameters of HNO/HON Calculated with Three DFT Methods with the 6-311++G Basis Set[a]**

	HNO			HON		
method	H3N1	N1O2	∠H3N1O2	H4O2	N1O2	∠H4O2N1
B3LYP/6-311G(2d,2p)[13]	1.063	1.201	108.4	0.997	1.257	111.6
B3LYP/6-311++G**	1.064	1.200	108.9	1.002	1.254	112.8
B3P86/6-311++G**	1.064	1.195	108.9	1.000	1.247	112.7
B3PW91/6-311++G**	1.065	1.195	109.0	1.001	1.247	112.8
ref 50	1.063	1.212	108.6			

[a] Bond lengths in Å and angles in deg.

TABLE 2: The Gibbs Free Energies (in kcal·mol^{-1}) of the Dissociation Reactions Calculated with Three DFT Methods and the 6-311++G Basis Set[a]**

reaction	B3LYP	B3P86	B3PW91	ref 51
HNO → H + NO	42.97	48.13	44.58	
HON → H + NO	5.19	7.00	3.26	
HNO → $H^+ + NO^-$	348.82	353.32	353.27	354.70 ± 0.40
HON → $H^+ + NO^-$	311.04	312.20	311.96	

TABLE 3: B3PW91/6-311++G Calculated Frequencies (cm^{-1}) of the Separated and Complexed Reactants HNO + H_2O and Products HON + H_2O**

	HNO + H_2O	AR	HON + H_2O	AP
ν_{as}(OH)	3960.7	3943.6	3960.7	3920.0
ν_s(OH)	3853.0	3816.4	3853.0	3471.9
ν(N1H3)	2874.4	2985.9		
ν(O2H4)			3089.9	2977.5
ν(NO)	1703.8	1703.8	1308.4	1422.9
δ(H5O4H6)	1604.8	1602.1	1604.8	1608.7
δ(HNO) in plane	1569.8	1598.9		
δ(HON) in plane			1490.3	1574.0
δ(HNO) out of plane		355.3		
δ(HON) out of plane				821.5
ν intermol		390.0		748.8
ν intermol		274.1		447.5
ν intermol		174.3		331.7
ν intermol		145.4		292.9
ν intermol		131.0		241.3

TABLE 4: The Binding Energies (kcal/mol) of Group A−E Complexes Calculated at the B3PW91/6-311++G + ZPE Level**

complex code	project	binding energy
AR	W1+R-AR	1.99
BR	W2+R-BR	3.54
CR	W32+R-CR	2.32
DR	W41+R-DR	2.09
ER	W42+R-ER	2.67
AP	W1+P-AP	7.78
BP	W2+P-BP	9.78
CP	W32+P-CP	8.76
DP	W41+P-DP	8.33
EP	W42+P-EP	9.69

has also been explored extensively by using different schemes on at least three low-lying PESs due to the importance in the nitrogen cycle.[11,32,33,35−39] The unambiguous isomerization activation energies are determined to be 72.9 kcal·mol^{-1} (at CCSD(T)/cc-pVTZ level) for the forward reaction and 41.2 (at B3LYP/6-311+G(2d) level) and 42.5 kcal·mol^{-1} (at CCSD(T)/cc-pVTZ level) for the backward reaction. Regarding these energy quantities, our calculated results at three DFT levels with a 6-311++G** basis set are collected in Tables 2 and 5. Together with geometrical parameters and vibrational frequencies given in Tables 1 and 3, the results determined here with DFT/6-311++G** methods have shown a good agreement with the corresponding experimental values and other theoretical values. Furthermore, the results of the two DFT methods, B3P86 and B3PW91, with the 6-311++G** basis set are almost the same at our calculational level. Also our CCSD(t,full)/6-311++G** results obtained at the B3PW91/6-311++G** geometries have confirmed the B3PW91/6-311++G** to be a reliable method. So we will use the B3PW91/6-311++G** method to discuss the properties of geometries and isomerizations.

TABLE 5: Relevant Energy Quantities (kcal·mol^{-1}) for HNO/HON and Group A−E Complexes Calculated with B3PW91/6-311++G + ZPE and CCSD(T)/6-311+G**// B3PW91/6-311++G** + ZPE[a]**

	ΔE_1	ΔE_2	ΔE_3
B3PW91			
HNO/HON	72.62	31.31	41.31
A(AT1)	38.49	2.97	35.53
A(AT2)	65.61	30.08	35.53
B	37.97	2. 90	35.07
C	37.32	2.44	34.88
D	37.32	2.25	35.08
E	36.85	2.55	34.30
CCSD(t,full)			
HNO/HON	71.95	29.13	42.82
A(AT1)	45.18	7.12	38.06
A(AT2)	69.06	30.99	38.06
B	42.01	5.30	36.71
C	40.80	3.59	37.21
D	43.09	5.46	37.63
E	42.87	6.14	36.73

[a] ΔE_1 is the forward barrier, ΔE_2 is the backward barrier, and ΔE_3 is the energy difference between the reactants and the product, viz. reaction heat. The same is true in other tables. The ZPEs are all calculated with B3PW91/6-311++G**.

Analysis about those investigations has indicated two important characteristics: (i) For the HNO/HON interconversion process there is a high barrier, which is by ∼25 kcal·mol^{-1} over the dissociation threshold on the singlet state ($^1A'$) PES. In contrast, only a small isomerization barrier exists on the low-lying triplet excited-state PES.[33] (ii) The isomerization reaction is spin-forbidden if it is to connect the ground states of HON ($^3A''$) and HNO ($^1A'$).[30,39] These observations have implied an alternative photochemical channel for the interconversion HNO/HON, which is presumably reached by the dissociation of the two isomers into NO radicals and H atoms[11] and then recombinations in the gas phase. Seemingly, this provides support for the nitrogen cycle, which relies on interconversion between HON and HNO isomers not only on the ground-state PES but also on the excited-state PESs.[33]

However, all these data and analyses mentioned above are limited to the gas phase process only although they have provided very much valuable information. Obviously, they could not apply to the processes in solution and in the biological systems. It is well-known that there are many water molecules in both biological systems or the atmosphere, so it can be predicted that the coupling interaction of explicit water molecules with HNO/HON must play a very important role in catalyzing this interconversion. However, these kinds of works are relatively scarce, and to our best knowledge, no systemic

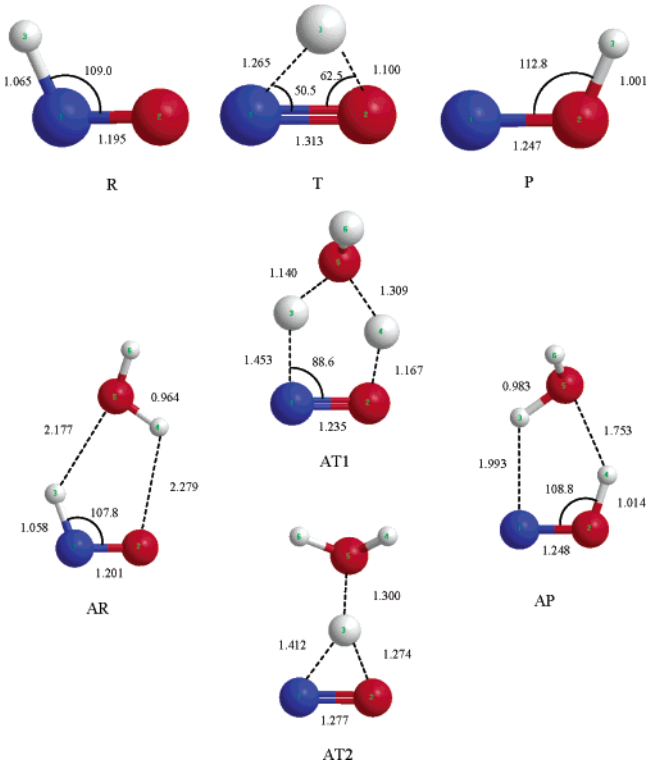

Figure 1. Geometries of the stationary points for the isolated PT-isomerization (HNO (R) and HON (P) monomers, and transition state T) and for the monohydrated PT-isomerization reactions (two transition states, AT1 and AT2) determined at the B3PW91/6-311++G** level. Bond lengths are in angstroms and angles in degrees. The red, blue, and gray balls denote the oxygen, nitrogen, and hydrogen atoms, respectively. These designations also apply to the other figures.

conclusion has been drawn. Therefore, a detailed theoretical analysis regarding explicit water assisting HNO/HON isomerizations is given in the following sections.

3.2. One-Water-Assisting Proton-Transfer Isomerization. *3.2.1. Geometrical Character. a. Stable States of Species Looped with One Water.* For the monohydrated species, geometrical optimizations have found two stable states on the global PES. Frequency analysis indicates that they are genuine minima. More interesting is that each of them (HNO, HON) is looped with one water molecule. No single-site coupling modes have been found. The optimized geometrical parameters of the monohydrated HNO (AR) and the monohydrated HON (AP) are displayed in Figure 1, together with those of HNO (R) and HON (P) for comparison.

In each AR and AP complex, the H_2O molecule forms two hydrogen bonds with the HNO or HON. The atoms (N1, O2, H3, H4, and O5) participating in the proton-transfer process are almost coplanar, and the atom H6 is out of this plane.

The *r*(N1O2) is 1.201 Å in the complex AR, slightly longer than that (1.195 Å) in the unhydrated HNO (R). So it can be seen that the participation of the H_2O molecule weakens the N1O2 bond but the N1H3 bond is slightly strengthened, because their lengths are 1.065 Å in molecule R and 1.059 Å in the complex AR, respectively. However, comparing the complex AP with molecule P, the O2H4 bond is elongated by 0.013 Å, while the length of the N1O2 bond hardly changes.

Further, attachment of another water molecule to the atom H6 may yield the complexes BR and BP (displayed in Figure 2). The five atoms (N1, O2, H3, H4, and O5) that participate in the proton-transfer process are also coplanar. More interesting is that the addition of the second water as a side chain has

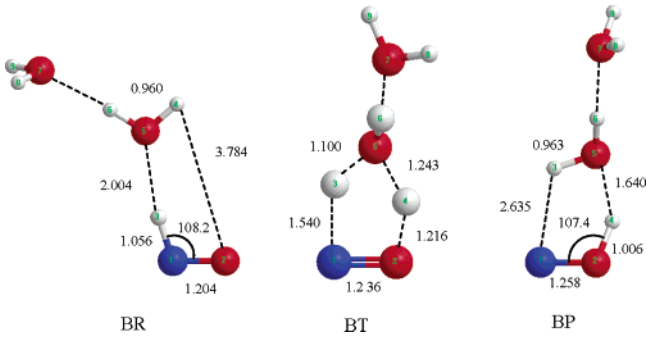

Figure 2. Geometries of the stationary points for the PT-isomerization reaction with one water molecule participating and one water molecule assisting determined at the B3PW91/6-311++G** level. Bond lengths are in angstroms and angles in degrees.

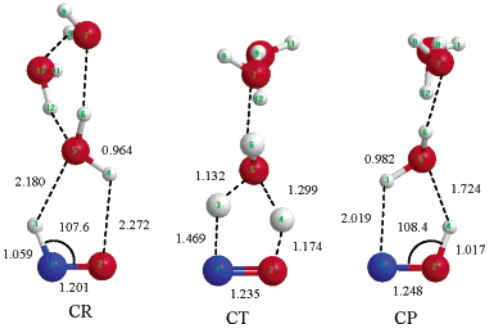

Figure 3. Geometries of the stationary points for the PT-isomerization reaction with one water molecule participating and two water molecules assisting determined at the B3PW91/6-311++G** level. Bond lengths are in angstroms and angles in degrees.

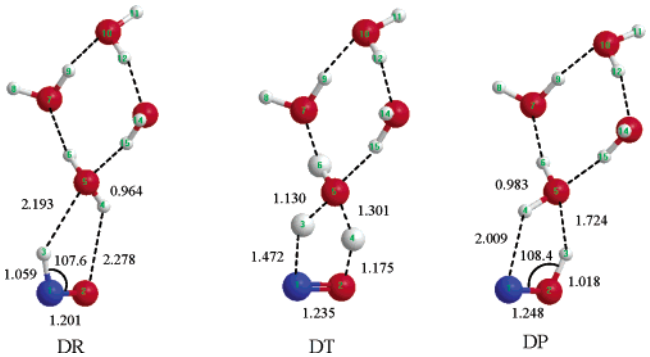

Figure 4. Geometries of the stationary points for the isomerization reaction with one water molecule participating and three water molecules (structure 1) assisting determined at the B3PW91/6-311++G** level. Bond lengths are in angstroms and angles in degrees.

significantly affected the H4O2 hydrogen bond in the complex BR, making it 3.784 Å, being considered broken. Another reason for the rupture of the hydrogen bond O2H4 can be found from the analysis of the Mulliken charge. The charge of the atom O4 in the complex BR is −0.662 e, while in the complex AR it is −0.543 e. A similar change is not found in complex BP compared to complex AP when one more H_2O molecule is added and the charge of the atom O5 varies from −0.559 e to −0.691 e.

When two H_2O molecules are added to the complexes AR and AP, the complexes CR and CP can be obtained, while adding three H_2O molecules to AR and AP may form the complexes DR, ER, DP, and EP. Theses are displayed in Figures 3−5. The complexes ER and EP also can be found when one more water molecule is attached to the atom H9 in the complexes CR and CP, respectively. From these it can be seen

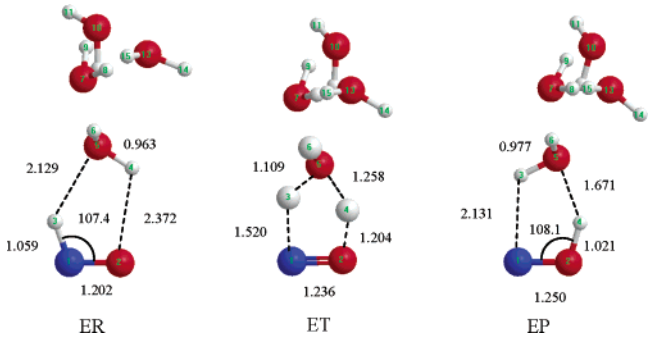

Figure 5. Geometries of the stationary points for the isomerization reaction with one water molecule participating and three water molecules (structure 2) assisting determined at the B3PW91/6-311++G** level. Bond lengths are in angstroms and angles in degrees.

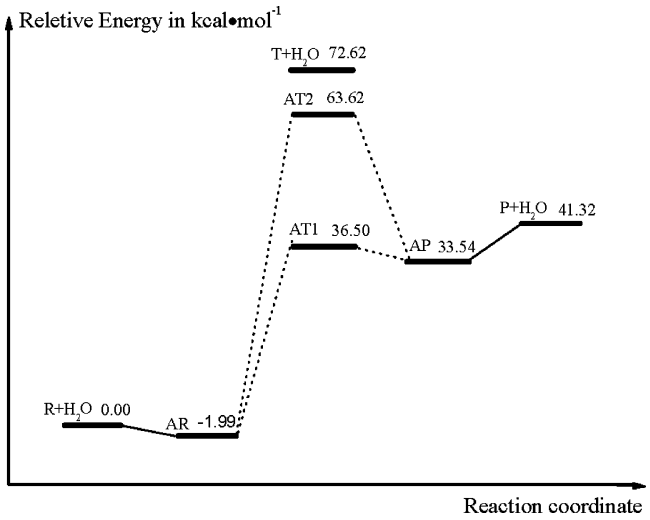

Figure 6. Reaction profile for the monohydrated reactions calculated at the B3PW91/6-311++G** level with the ZPE. The energies are defined with respect to the molecule HNO (R) + H_2O (in kcal·mol^{-1}).

that the atoms N1, O2, H3, H4, and O5 are also basically coplanar in the four complexes. The atom H6 is out of the plane at about the same directions as it in complexes AR and AP.

The lengths of the hydrogen bonds H3O5 and H4O2 in the complexes AR, CR, and DR and those of H3N1 and H4O5 in the complexes AR, CP, and DP clearly have not been altered. The biggest discrepancy is in the H3N1 bonds in the complexes AP and CP, only 1.3%. This is because there are trimolecular or quadrimolecular water loops in the complexes CR, CP, DR, and DP, and the added water group is not only an electron donor but also an electron acceptor to HNO/HON. That is to say on one hand the group contributes an electron to the atom H6 and on the other hand it accepts an electron from the atom O5; this cooperation causes no significant change of the charge population of the atoms in the proton-transfer loop.

The calculated frequencies for isolated molecules and complexes AR and AP are given in Table 3. The frequency shift for the N1H3 stretching mode in the AR complex with respect to that in the HNO monomer is 111.5 cm^{-1}, a blue-shift, while that for the O2H4 stretching mode in the AP complex with respect to the HON monomer is −112.4 cm^{-1}, a red-shift. In the AR complex, because of the emergence of the two hydrogen bonds, the electronic cloud has been redistributed. In this complex, the atoms O5 and O2 are electron donor sites to the atoms H3 and H4, and the atom N lacks an electron for the connection with the atom O2 and the electronegativity of element O is bigger than that of element N, so the result of this cooperation is that the net charge of the atom N1 changes from −0.163 e to −0.177 e, while that of the atom H3 increases from 0.180 e to 0.238 e. As a result, the ν(N1H3) has a blue-shift, and is not the same as the situation for the traditional hydrogen bond. In the complex AP, the atom O2 connected with the atom N1 is electron rich, so under the same effect mentioned above about complex AR and for the traditional hydrogen situation, the ν(O2H4) has an an obvious red-shift.

In addition, it should be noted that (i) the ν_{as}(OH) and the ν_s(OH) in the complex AP are different from those in complex AR, viz. the ν_{as}(OH) may be mostly assigned as the vibration of the bond O5H6, while the ν_s(OH) mostly is referred to as the vibration of the bond O5H3. These are different from those in the complex AR, and because of the restraint of the hydrogen bond N1H3, the ν_s(OH) is red-shifted. (ii) Comparison between the atom H4 linked with atomic group N1O2 in complex AP and the atom H3 in complex AR has indicated a blue-shift.

b. Transition States. The AT2 transition state is characterized by an interaction between the water oxygen and the migrating hydrogen of HNO, and its geometry is displayed in Figure 1. The reaction vector corresponds to H transfer between N and O atoms, and the associated frequency is 1928.7i cm^{-1}. The atom H3 migrates from the N1 fringe to the approximate center of the atoms N1, O2, and O5 with the help of the water molecule H6O5H4. Obviously, this mechanism is very similar to that in the free state case, but the transferring H-atom is loosely bound to the NO molecular fragment due to the coupling interaction from one water.

The AT1 transition state is characterized by a five-membered cyclic structure like the AR and AP, and its geometry is also presented in Figure 1. This mechanism is obviously different from the AT2 mechanism. The latter (AT2) is a direct proton-transfer path, but the former is an indirect intracyclic proton translocation instead of a direct pathway. In going from the reactant AR to this transition state, the fragment H4O5H6 approaches the fragment H3N1O2, and the bonds H3N1 and O5H4 are going to be broken, while the bonds O5H3 and O2H4 are going to be formed. Another point that can be found from the geometry is that the transition state AT1 is closer to the product AP than to the reactant AR. This observation also can be proved from the energetic aspect mentioned below. The reaction vector consists of a concerted rocking motion of H3 and H4 between N1, O5 and O2, O5, respectively, and the associated frequency is 1436.8i cm^{-1}. Consequently, along this path, AR-AT1-AP, a proton exchange between HNO and H_2O occurs. The intrinsic reaction coordinate (IRC) scan also proves this mechanism.

Similarly, the transition states BT, CT, and DT (displayed in Figures 2, 3, and 4) are correlative to the reactants and products of their groups, respectively. Their geometries are similar to the transition state AT1, and will not be discussed in detail here.

3.2.2. Energetic Aspect. a. Proton-Transfer Isomerization in Mono-Water-Looped Systems. Figure 6 shows the reaction profile for the one-water-assisting proton-transfer reactions calculated at the B3PW91/6-311++G** level with the ZPE correction. The binding energy between HNO and H_2O is 1.99 kcal·mol^{-1} for the complex AR, and that between HON and H_2O is 7.78 kcal·mol^{-1} for the complex AP. The reactant and product complexes (AR and AP) of the AT1 and AT2 pathways coincide with the thermodynamic complexes AR and AP on the PES (shown in Figure 7).

The monomolecular isomerization reaction without water-assisting is endothermic by 41.32 kcal·mol^{-1} whereas the endothermicity of the monohydrated reaction (path AT1 or AT2)

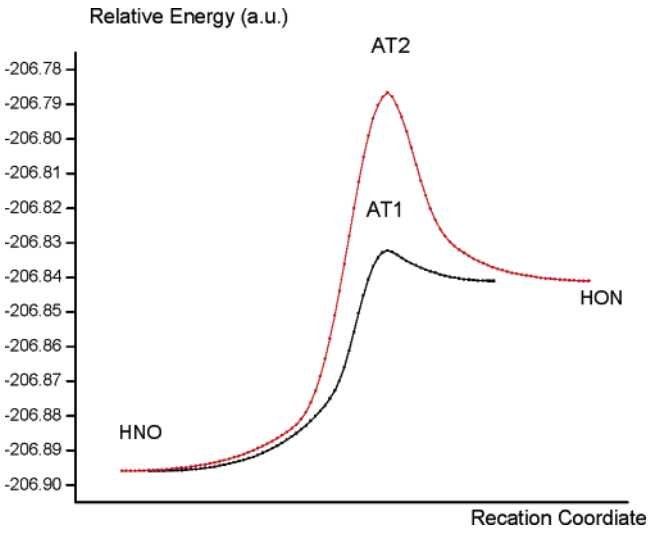

Figure 7. Energy profiles along the reaction paths AT1 and AT2 at the B3PW91/6-311++G** level.

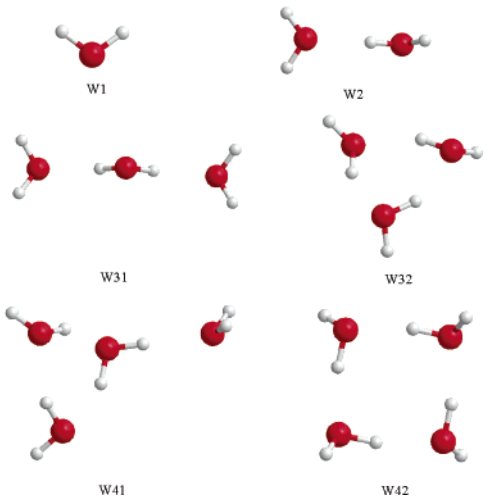

Figure 8. Geometries of the stationary points for the isolated water complexes that were used in calculating the binding energies.

is reduced to 33.54 or 35.53 kcal·mol^{-1} when we consider (R + H_2O) or the complex AR as the reactant, respectively. The endothermicity is reduced because of the large binding energy of the complex AP, which is about three times the corresponding energy for the complex AR. The resulting interaction with one water molecule, therefore, has an important effect on the relative stability between the reactant AR and the product AP.

Starting from the complex AR, there exist two distinct pathways leading to the same final complex AP. The activated vibrational modes determine whether reaction occurs via AT1 or AT2. When all modes are equally activated, the channel with the smallest activation energy is more likely. The transition state is placed at 72.62, 63.62, or 36.50 kcal·mol^{-1} above the separated species R + H_2O for the unhydration assisting isomerization and for monohydration pathways AT2 and AT1, respectively. This comparison reveals that a large stabilization is brought about by one more hydrogen bond existing in the pathway AT1.

b. Relative Energy of Groups A−E. i. Binding Energy. All of the binding energies were calculated at the B3PW91/6-311++G** + ZPE (zero-point energy). The binding energies of the complexes of groups A−E are collected in Table 4. The energies of water molecules used here to calculate the binding energies of the complexes of groups B−E are not the sum of the energies of several water molecules but the energies of the corresponding water polymers (displayed in Figure 8). Only in this way can we find the natural capability of the HNO and the HON to associate with these water molecular clusters. The binding energies of the complexes of group B are bigger than those of groups A and C, because of the enlargement of the angles ∠O5H3N1 and ∠O5H4O2 in the complexes BR and BP, respectively. So the tension of the reaction loop becomes smaller, and the stability of group B complexes is greater than that of groups A and C. Further, it can also be seen that the biggest changes of the binding energies of the complexes of groups C−E are 0.68 kcal/mol, and those of HON are 1.91 kcal/mol, respectively, when the number of out-of-loop water molecules changes from zero (in the complexes AR and AP) to three (in the complexes DR, DP, ER, and EP). It shows that the binding energy does not change obviously with augmentation of out-of-loop water molecules when one water molecule assists the HNO/HON isomerization via forming a one-water-containing loop, because the binding energy calculated here is only the energy of the two hydration bonds between the molecule HNO/HON and the water cluster.

ii. Activation Energy. The activation energies of group A and the unhydrated system have been discussed above. There is a little decrease in the reaction energies of the other four groups with the additional water molecules. From the relative energies calculated with B3PW91/6-311++G** of groups B−E (listed in Table 5), compared with group A (path AT1), the forward reaction barriers are reduced slightly by 0.52, 1.17, 1.17, and 1.64 kcal·mol^{-1} in groups B−E, while the corresponding energy barriers of the backward reaction are reduced slightly by 0.07, 0.53, 0.72, and 0.42 kcal·mol^{-1}, respectively. The relative energies calculated with CCSD(T)/6-311+G**//B3PW91/6-311++G** of groups A−E compared with the energies calculated with B3PW91/6-311++G** are also listed in Table 5. We can see that the reaction trend of all of these groups is consistent although the values have slight deviations between them due to the geometries optimized at the non-CCSD(t,full) level. So we will use the energies calculated with B3PW91/6-311++G** in the remainder of the discussions for the purpose of saving the calculating time, although the B3PW91 method is not such a high level theory as the CCSD(t,full) method.

Therefore, a conclusion can be drawn that the additional more out-of-loop water molecules do not have an obvious impact on the mono-water-assisting isomerization. In the following, we will continue to discuss whether the out-of-loop water molecules do have a small effect on the reaction energy or not for other situations.

3.3. Two-Water-Assisting Proton-Transfer Isomerization. From section 3.2, it can be found that there are strong consequences in the mono-water-assisting isomerization of HNO/HON compared to the unhydration-assisting one: barrier lowering and also a decrease in the reaction energy. Especially for the in-loop water molecule, the catalytic effect is more obvious. So it is interesting to find whether the isomerization barrier is lowered more or not when there are more out-of-loop water molecules for assisting. Further, we are first interested in that if two water molecules and HNO/HON form the isomerization loop (the proton-transfer loop), how do the systems change? Figure 9 shows the geometries and parameters of the stationary points for the HNO/HON isomerization reaction with two in-loop water molecules for assisting.

3.3.1. Geometries. a. Complexes The two water molecules form two hydrogen bonds with the monomer HNO/HON, and one inner hydrogen bond between themselves in complexes FR

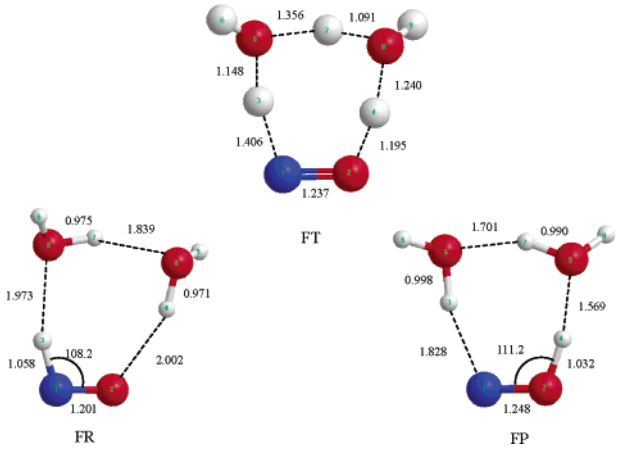

Figure 9. Equilibrium geometries of the dihydrated structures determined at the B3PW91/6-311++G** level. Bond lengths are in angstroms and angles in degrees.

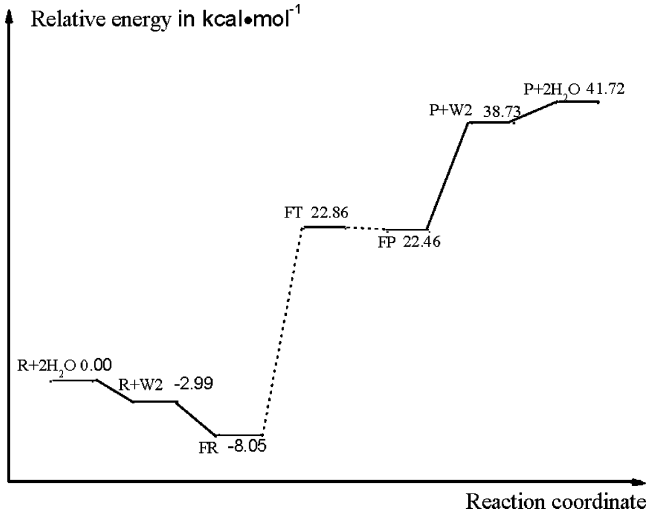

Figure 10. Reaction profile for the dihydrated reactions calculated at the B3PW91/6-311++G** level with the ZPE. The energies are defined with respect to the HNO (R) $+2H_2O$.

and FP. All the atoms which directly participate in the isomerization are almost coplanar. For the convenience of discussion, we refer to this plane as the reaction plane and the loop as the reaction loop as we have done in section 3.2. The atoms H6 and H9 are out of this plane in opposite directions (cf. Figure 9).

The *r*(N1O2) is 1.201 Å in the complex FR, and this value is equal to that in the complex AR. The bond N1H3 is strengthened, just like that in the complex AR. In the complex FP the bond O2H4 is slightly elongated, from 1.014 Å to 1.032 Å, compared to that in the complex AP. This has been demonstrated from the charge distribution. In the complex AP the net charges of atoms O2 and H4 are 0.093 e and 0.313 e, respectively, and in the complex FP those are 0.004 e and 0.424 e, respectively. The electron cloud density of the atom O2 is increased and that of the atom H4 is decreased, and as a result the interaction between the atoms O2 and H4 is weakened. So the *r*(O2H4) is longer in the complex FP than that in the complex AP. The value of the angle ∠H3N1O2 in the complex FR is closer to that in the complex R than that in the complex AR. There exists such a trend in every molecule participating in forming the hydrated complex that it could contain its slack geometry in such a weak interaction system. In the complex AR, the value of the angle ∠H3N1O3 is much less than that of its slack state, because two hydrogen bonds are formed between the water molecules and the HNO molecule and the sum of all the internal angles should be 540° or so in this similar pentagon. While in the complex FR there is a heptagon formed by the reaction-participating atoms so the homologous angles could be slacker than those in the complex AR, the value of the angle ∠H3N1O2 is closer to that in the complex R (its slack state). The variation of the angle ∠H4O2N1 in the complexes R, AR, and FR has the same rule as above.

We get group G by linking one water molecule with the atom H6 in the complexes of group F, group H by linking one water molecule with the atom H9, group I by linking two water molecules with the atoms H6 and O5, group J by linking two water molecules with the atoms H6 and H9, respectively, and group K by linking two water molecules with the atom H9 and O8. The Cartesian coordinates of the complexes of these four groups and the corresponding geometries can be found in Table S1 and Figures S1−S8 in the Supporting Information. The atoms of the reaction loop are almost coplanar in the reactants and products of groups F−K (see Table S2 in the Supporting Information). The directions of the other H atoms out of the plane are not important to the isomerization, so they will not be discussed any more here. The bonds N1O2 and the angles ∠H3N1O2 have almost the same values in each reactant of groups G−K as those in the complex FR, and the same rule can be found in the values of the bond N1O2 and those of the angles ∠H4O2N1 in the product of group G−K complexes compared to those in the complex FP.

The added one more water molecule (H11O10H12) is a pure electron donor in the complex GR, so the net charge of the atom O5 varies from −0.619 e to −0.712 e compared to that in the complex FR. This variation causes the atom O5 to attract the H atom around it tightly. So the bond lengths (O5H3) and (O5H7) decrease, while the bond lengths (N1H3) and (O8H7) increase. A similar phenomenon can be found in the complexes GP, HR, and HP. The behavior of the added two water molecules in the complexes IR, KR, IP, and KP is the same as that in the complexes CR, CP, DR, and DP and will not be discussed any more here. The added two more water molecules (H11O10H12 and H14O13H15) in the complexes JR and JP are both pure electron donors, so it can be seen that the bonds O5H3 and O8H4 are strengthened, but the bonds N1H3 and O2H4 are weakened.

From all of the above, it can be concluded that the attachment of more out-of-loop water molecules to the in-loop water molecules can enhance the hydrogen bonds between the water molecules and the HNO/HON molecule.

b. Transition States. All of the atoms of the reaction loop in the transition states of groups F−K are almost coplanar, and this can be demonstrated by the correlative dihedral angles (cf. Table S3 in the Supporting Information).

In the transition state FT, the simultaneous motions of the three in-plane hydrogen atoms have been identified as the reaction vector (N1···H3···O5, O5···H7···O8, and O8···H4···O2) and the associated frequency is 1218.0i cm^{-1}. The transition state structure FT is similar to the AT1 with an additional water molecule taking part in the cyclic arrangement.

A similar situation can be found in the transition states of groups G−J and T, and only the hydrogen bond lengths have a little difference due to the addition of more water molecules.

3.3.2. Energetic Aspects. a. Dihydrated Isomerization. Figure 10 shows the reaction profile for the two in-loop waters assisting reactions calculated at the B3PW91/6-311++G** level with the ZPE. It can be seen that the energy of conjunction of two water molecules is −2.99 kcal·mol^{-1} and the binding energy

TABLE 6: The Binding Energies of Group F−K Complexes at B3PW91/6-311++G + ZPE**

complex code	project	binding energy
FR	W2+R-FR	5.06
GR	W31+R-GR	6.33
HR	W31+R-HR	7.20
IR	W42+R-IR	4.71
JR	W42+R-JR	1.47
JR[a]		4.45
KR	W42+R-KR	4.93
FP	W2+P-FP	15.87
GP	W31+P-GP	17.51
HP	W31+P-HP	19.00
IP	W42+P-IP	15.72
JP	W42+P-JP	13.49
JP[a]		16.47
KP	W42+P-KP	16.18

[a] The energies are corrected with the binding energy of complex W2.

TABLE 7: Relative Energies (kcal·mol^{-1}) for the Complexes of Group F−K Calculated with the 6-311++G Basis Set in the B3PW91 Method + ZPE**

group	ΔE_1	ΔE_2	ΔE_3
F	30.91	0.40	30.51
G	30.56	0.42	30.14
H	29.31	−0.20	29.52
I	30.56	0.25	30.31
J	29.34	0.05	29.29
K	30.05	−0.01	30.06

of the complex FR is −5.06 or −8.05 kcal·mol^{-1} when we consider whether the two water molecules link up or not.

If the complex FR is considered as the reactant of the isomerization reaction and the complex FP as the product, the isomerization is endothermic by 30.51 kcal·mol^{-1}. Compared with those of the unhydrated species and group A, the heat absorption of the isomerization reaction is reduced more. The forward and the backward barriers of the isomerization have been reduced to 30.91 and 0.40 kcal·mol^{-1}, respectively.

b. Relative Energy of the Complexes of Groups F−K. i. Binding Energy. The binding energies of the complexes of groups F−K are given in Table 6 calculated at the B3PW91/6-311++G** level with the ZPE correction. Some details for calculating the binding energies should be pointed out: first, we could not find a proper single stabilization state of the proper water molecule alignment corresponding to those in the complexes GP and HR, so we used the energy of the complex W2 in calculating the approximate binding energies of both of them; second, the most stable states of the water molecule alignments in the complexes JR and JP have not be found either.

Table 6 indicates that the hydration energies of the HON-derived products of all of the groups are larger than those of the corresponding reactants. The binding energies of the relevant complexes of groups I−K have unmoral differences: the binding energies (data on the first line) of the group J complexes are much smaller than those of the relevant group I and K complexes. This may be due to the fact that the energy of the complex W42 is used to calculate the binding energy of group J, and there is a deviation in their binding energies since the complex W42 has one more hydrogen bond than the water molecule alignment in the complexes of group J. Therefore, the energy of one normal water−water hydrogen bond should be added into the binding energies of the complexes JR and JP, and the binding energy of the complex W2 is appropriate to use as the energy of one normal water−water hydrogen bond. Adding the binding energy of the complex W2 to the binding energy of the complex of group J, we can obtain the energies of the group J complexes, as listed in the second line of JR and JP data in Table 6. Comparison reveals that the binding energies of the group J complexes after correction are not obviously different from those of the group I and K complexes, only with a little deviation because of the difference of the water molecule alignment.

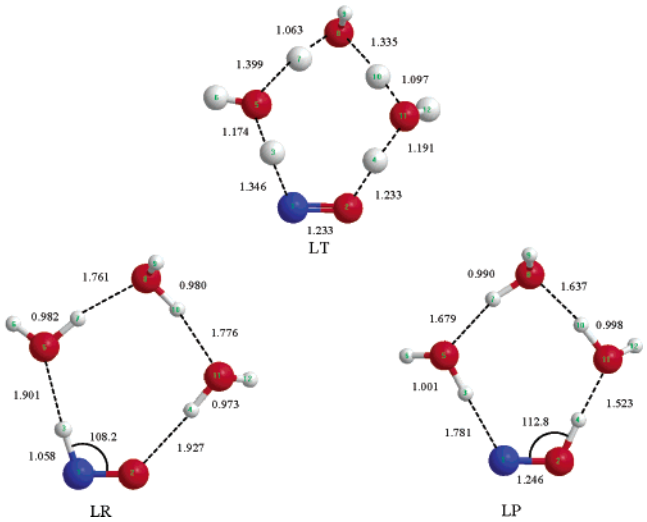

Figure 11. Geometries of the stationary points for the isomerization reaction with three water molecules participating determined at the B3PW91/6-311++G** level. Bond lengths are in angstroms and angles in degrees.

ii. Activation Energy. The reaction heat, the forward barrier, and the backward barrier do not vary obviously when two in-loop water molecules assist the isomerization with the number of out-of-loop water molecules going from zero to two (listed in Table 7). For example, the energies of the forward barriers of the isomerization vary between 29.31 and 30.91 kcal·mol^{-1}, and the increment is only 1.6 kcal·mol^{-1}. The reactant of group I has one more water molecule than that of group G, but the energies of the forward barriers of the isomerization of the two groups are the same at our calculational level.

For these systems, it should be noted that there are several negative values in the energies of the backward barriers at our calculational level, probably because there exists positive deviation when DFT (density function theory) is used to calculate the effect of the hydration bonds, and the transition states have several more hydration bonds than the products. Thus the positive deviation of the energies of the transition states is bigger than those of the products, which cause the backward barriers to be negative partially. The same phenomena can be found in the next section and it would be improved by using more accurate methods.

3.4. Three and Four In-Loop Water Molecules Assisting Proton-Transfer Isomerization. The isomerization is further studied with three and four water molecules in the reaction loops. A reactant complex, LR or PR, and a product, LP or PP, are connected to a transition state, LT or PT, and the corresponding geometries are displayed in Figures 11 and 12. The complexes that involve more than four water molecules will not be considered in this paper. For three-water looped systems, we can obtain three groups (M, N, and P) of isomers when adding one water molecule to the atoms H6, H9, and H12 of the complexes of group L, respectively. We have ensured that the eigenvalue of the respective Hessian corresponds to the transfer of the H atoms between the atoms N and O along the water chains in all five transition states. Reaction profiles of groups

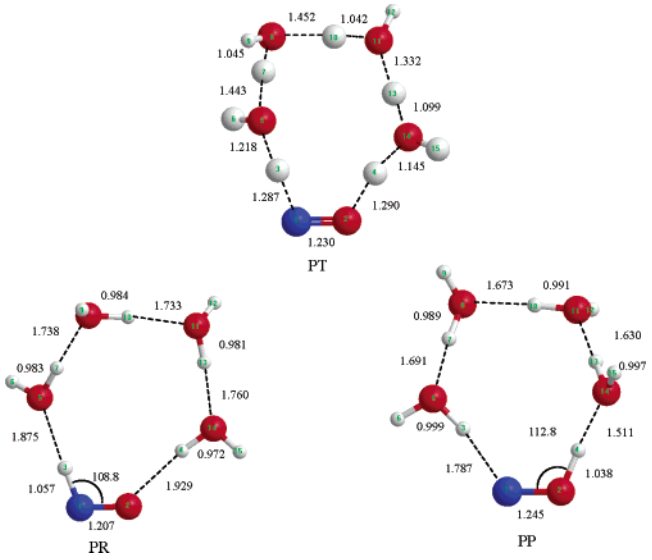

Figure 12. Geometries of the stationary points for the isomerization reaction with four water molecules participating determined at the B3PW91/6-311++G** level. Bond lengths are in angstroms and angles in degrees.

TABLE 8: The Hydrogen Bond Lengths (Å) of the Reactants and the Products in Groups L−P

	reactants		products	
hydrated bonds	O5H3	O2H4	N1H3	O11H4
group L	1.901	1.927	1.781	1.523
group M	1.832	1.919	1.851	1.527
group N	1.888	1.951	1.794	1.493
group O	1.908	2.005	1.762	1.449
group N	1.875	1.929	1.787	1.511 (O14H4)

TABLE 9: The Hydrogen Bond Lengths (Å) of the Reactants and the Products in Groups B, F, L, and P

	reactants		products	
hydrated bonds	O5H3	O2H4	N1H3	XH4
group B	2.177	2.279	1.993	1.754 (X = O5)
group F	1.973	2.002	1.828	1.569 (X = O8)
group L	1.901	1.927	1.781	1.523 (X = O11)
group P	1.875	1.929	1.787	1.511 (X = O14)

L and P are presented in Figure 12 and will be discussed in the next section for comparison with the unhydration, monohydration, and dihydration assisting isomerizations.

3.4.1. Geometries. a. Complexes A cyclic structure resulting from the interaction of HNO or HON with a chainlike water cluster can be found in each of the reactants and products of groups L−P. The dihedral angles of the atoms H4, O5, H7, O8, H9, and O11 with respect to the plane O2N1H3 in the complexes of groups L−O are all not more than 5°. The analogous dihedral angles (can be found in Table S5 in the Supporting Information) in the complexes PR and PP show different phenomenon from all the complexes of groups A−O. The biggest dihedral angle is about 20° with respect to the plane O2N1H3, and the reason will be discussed in section 3.5.

The bond lengths of the hydrogen bonds that directly link with HNO or the HON in the reactants and products of groups L and P are listed in Tables 8 and 9 and the same mutative rule as the above could be found.

b. Transition States. The simultaneous motions of the hydrogen atoms in the reaction loop have been identified as the reaction vector that corresponds to the proton transfer in all five transition states and the associated frequencies of the transition states of groups L−P are 1068.3i, 1138.5i, 928.9i, 727.9i, and 885.3i cm^{-1}, respectively.

Every one of the dihedral angles of the atoms in the reaction loops with respect to the plane H3N1O2 is smaller than 5° in the transition state LT, MT, NT, and OT, which correspond with their homologous reactant and product. The values of the dihedral angles of the heavy atoms O5, O8, O11, and O4 with respect to the plane O2N1H3 in the transition state PT are 0.6°, 19.3°, 11.4°, and −2.8°, respectively. We consider that the atoms in the reaction loop are not coplanar in the transition PT.

TABLE 10: The Binding Energies (kcal·mol^{-1}) of the Reactants and Products of Groups L−P at B3PW91/6-311++G + ZPE**

complex code	project	binding energy
LR	W31+R-LR	10.00
MR	W42+R-MR	4.64
NR	W42+R-NR	5.03
OR	W42+R-OR	5.76
PR	W41+R-PR	0.95
LP	W31+P-LP	22.42
MP	W42+P-MP	17.29
NP	W42+P-NP	17.92
OP	W42+P-OP	18.97
PP	W41+P-PP	13.97

TABLE 11: Relative Energies (kcal·mol^{-1}) for Group L−P Complexes Calculated with the 6-311++G Basis Set in the B3PW91 Method + ZPE**

group	ΔE_1	ΔE_2	ΔE_3
L	29.10	0.21	28.89
M	29.28	0.61	28.67
N	28.16	−0.27	28.43
O	27.56	−0.54	28.10
P	30.79	1.96	28.83

3.4.2. Energetic Aspects. a. Binding Energies. The binding energies of the reactants and products of groups L−P are collected in Table 10. The binding energy of the complex LR is about 5 kcal·mol^{-1} bigger than that of each one of the complexes MR, NR, and OR, and about 9 kcal·mol^{-1} bigger than that of the complex PR. The same phenomenon can be found in comparing the complex LP with the complexes MP, NP, OP, and PP. Further, it can be found that each complex of group L is more stable than any of the relevant complexes of groups M−P. That is to say the added one more water molecule can improve the stability of the complexe LR or LP no matter where the water molecule is added.

b. Activation Energy. The activation energies of groups L−P are also given in Table 11. The ΔE_1 (the forward barrier), ΔE_2 (the backward barrier), and ΔE_3 (the reaction heat) vary little, and their mutative ranges are 1.72, 1.05, and 0.57 kcal·mol^{-1}, respectively, when one more water molecule is attached to the atoms H6, H9, and H12 in group L, respectively. Comparing group L with group P, we can find that the reaction heat varies only 0.06 kcal·mol^{-1}, while the forward and backward energy barriers have increased 1.69 and 1.75 kcal·mol^{-1}, respectively. Considering the computational error, we can see that the reaction energy of the isomerization has reached a quite minor value and hardly changes when the number of water molecules in the isomerization reaction loop increases.

3.5. Comparison of the Different Proton-Transfer Isomerization Pathways. We have discussed the unhydration, monohydration, dihydration, trihydration, and tetrahydration in-loop assisting isomerizations of the HNO/HON system with different numbers of out-of-loop water molecules. From the above it can be seen that the out-of-loop water molecules have little effect on the isomerizations, and it will not be discussed any more

TABLE 12: The Angles (deg) of the Reactants and the Products in Groups A, F, L, and P

		group			
angle	optimal value	A	F	L	P
reactants					
∠H3N1O2	109.0	107.8	108.2	108.2	108.8
∠H4···O2−N1	109.5	101.0	123.4	131.0	135.2
∠H···O−H	109.5	85.6	101.7	118.3	128.1
			95.1	102.9	112.1
				110.0	110.2
					118.7
∠O···H−O(or N)	175.0	116.6	159.1	174.3	178.7
		128.8	154.9	170.0	177.6
			157.3	166.9	174.6
				177.3	176.3
					191.2
products					
∠H4O2N1	112.8	108.8	111.2	112.8	112.8
∠H3−N1···O2	109.5	88.6	111.9	121.1	125.3
∠H···O−H	109.5	79.3	91.8	109.8	118.7
			102.0	101.3	107.8
				117.5	112.6
					122.5
∠O···H−O	175.0	136.7	161.9	179.1	189.9
		126.3	153.1	164.5	174.4
			167.5	172.1	173.0
				180.8	177.0
					182.7

here. The number of water molecules assisting the isomerization in loop impacts the geometries and the energy aspects of the complexes and the isomerization pathways greatly.

3.5.1. Geometries. There is little variance in the homologous covalent bonds N1O2, N1H3, and H4O2 in all of the complexes of the four groups in which the water molecules participate in the isomerization via the loop structures and the biggest range of the two bonds is 0.024 Å.

The bond lengths of the hydrogen bonds that directly link with the HNO or HON molecules are listed in Table 9. With the addition of the water molecules in the loop from one to three, the lengths of the hydrogen bonds between the HNO/HON molecules and the water molecules have been reduced regularly. The interaction between the water molecules and the HNO/HON molecules enhances, while when the number of added water molecules is from three to four, the lengths of those analogous hydrogen bonds have not changed. The bond lengths of the bonds O5H3 and XH4 have been reduced by 0.026 and 0.012 Å, respectively, while those of the bonds O2H4 and N1H3 have increased. That is to say that the additional one more water molecule has enhanced the interaction between HNO/HON and the water molecules.

Similarly, for the bond angles in the reactants and products of these groups, the value of the ∠O4H3O1 in the complex W2 is 175.0°, so we could consider that the angle of the ∠OHO in the water cluster linking with one hydrogen bond (O···H) and one covalent bond (O−H) should optimally be 175.0°, and also the optimal values of the angles of the hydrogen bonds N···H−O or N−H···O should also be ca. 175°. We even consider that the angles where the O atoms are the center should be 109° also. Furthermore, we can find the optimal values of the angles ∠HNO and ∠HON from the complexes R and P are 109.0° and 112.8°, respectively. For the relevant angles in the complexes of groups A, F, L, and P given in Table 12, we found that with the addition of water molecules the values of ∠H3N1O2 in the complexes of groups A, F, L, and P are 108° or so and ∠H4···O2−N1 varies from 108.8° to 112.8°, approaching the optimal values we have supposed, while ∠O···H−O (or N) in the reactants varies from 111.6° and 128.8° in the monohydrated complexes and to 175.0° in the trihydrated and tetrahydrated complexes, in good agreement with the optimal values we have supposed. A similar situation for the ∠O···H−O angle has also been observed in the products. ∠H···O−H values in the reactants and products vary as ∠O···H−O with an increase of the number of the water molecules. Furthermore, we have found all the homogeneous angles in the complexes of groups L and P do not change greatly.

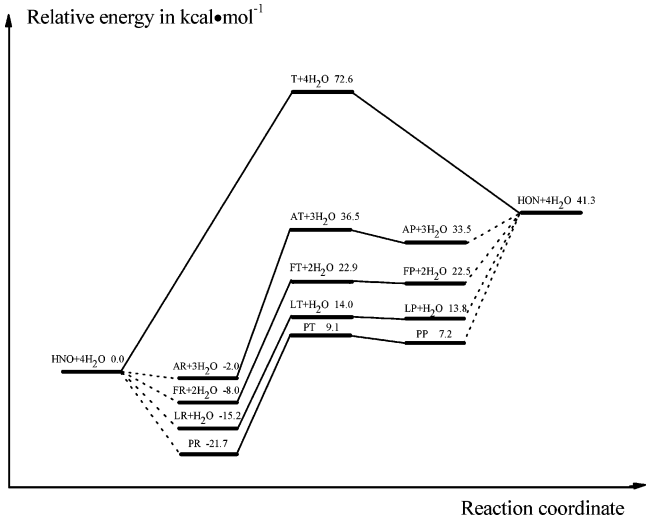

Figure 13. Reaction profiles for the monomolecular, monohydrated, dihydrated, trihydrated, and tetrahydrated pathways calculated at the B3PW91/6-311++G** level including the ZPE with respect to HNO + $4H_2O$.

From analysis of the bonds and angles, it can be seen that the HNO and HON molecules could contain their geometries well in the complexes, and the values of the covalent bonds OH in the water molecules are 0.960 Å or so and the variation range is less than 0.010 Å. ∠H4···O2−N1, ∠O···H−O (or N), and ∠H···O−H all vary to the optimal values approximately. So it can be predicted that the tension of the loop reduces with the addition of the number of water molecules. The values of all the homogeneous angles in groups L and P are at the same level, while some of the ∠O···H−O (or N) values are even greater than 180°. That is to say, there exists an inner tension in the reaction loop. This kind of tension is not favorable to the stability of the loop. This point can even be found from the dihedral angle analysis. When the HNO/HON is associated with one to three water molecules, the atoms of the loop could be approximately coplanar, and the biggest value of the dihedral angles is not more than 5°. However, the values of some dihedral angles vary to 20° or so in the complexes of group P, thus it can be concluded that the plane could not contain one more water molecule as it does in the complexes of group L. The plane has been distorted, and is not favorable to the stability of the system. But the values of the homogeneous angles and the bonds in the complexes of groups L and P are all close to the optimal values, so we think the geometries of the complexes of groups L and P are more suitable to isomerization than those of groups A and F.

3.5.2. Energetics. The reaction profiles for the unhydration, monohydration, dihydration, trihydration, and tetrahydration pathways of the HNO/HON isomerization are displayed in Figure 13. Figure 14 shows the variation trends of the forward barrier, the backward barrier, and the reaction energy with the increase of the number of the water molecules from zero to four. Starting from the respective reactant complex the required

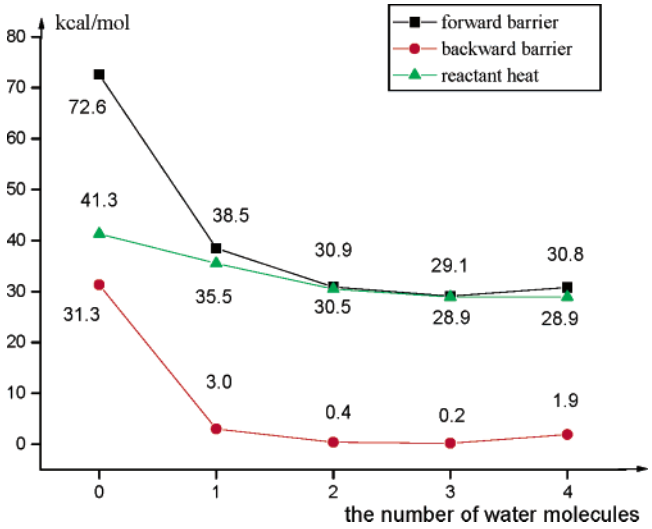

Figure 14. The variation trends of the forward barrier, backward barrier, and reactant heat with the increase of the number of the water molecules that participate in the isomerization. Calculated at the B3PW91/6-311++G** level with ZPE.

energies to overcome the barriers T, AT1, FT, LT, and PT are 72.6, 38.5, 30.9, 29.1, and 30.8 kcal·mol^{-1}. Thus, it can be seen that the unhydration-assisting isomerization (HNO → HON) barrier 72.6 kcal·mol^{-1} is lowered by 34.0 kcal·mol^{-1} with monohydration assisting, whereas dihydration, trihydration, and tetrahydration assisting bring further lowerings of the barriers by 7.6, 9.4, and 7.7 kcal·mol^{-1}, respectively. The activation energies for the isomerization of HON series from the complexes AP, FP, LP, and PP are 3.0, 0.4, 0.2, and 0.9 kcal·mol^{-1}, and the lowerings compared to the unhydration assisting situation are 28.3, 30.7, 31.2, and 29.4 kcal·mol^{-1}, respectively. The energies of the HNO/HON isomerizations are optimal when two, three, or four waters assist it, and the trihydration pathway is the best of the three.

4. Conclusion

We have studied some water-assisting pathways for the HNO/HON isomerization on singlet state PES by using 1−4 water molecules to loop HNO/HON. The effect arising from *n* out-of-loop water molecules is also examined by attaching the additional water molecules to the in-loop waters as the side chains. The total number of used waters is limited to not more than 4. For the monohydration pathways, there are two five-membered cyclic structures which correspond to the stable reactant and the product, and they may be interconverted via two transition states AT1 (with an in-loop water) and AT2 (with an out-of-loop water) with activation energies of 38.5 and 65.6 kcal·mol^{-1} at the B3PW91/6-311++G** level. Compared with the unhydration case T (72.61 kcal·mol^{-1}), the forward activation energies are decreased by 34.1 and 7.4 kcal·mol^{-1}, and the homologous backward values are also lowered by 1.2 and 28.3 kcal·mol^{-1}. The corresponding reaction heat is 35.5 kcal·mol^{-1}, being smaller by ~6.0 kcal·mol^{-1} than that (41.3 kcal·mol^{-1}) of the unhydrated case. The influence of the out-of-loop waters is also examined with not more than three water molecules. On the basis of the AT1 mechanism, attachment of 1−3 water molecules to the in-loop water as the side chains may cause the activation energies and reaction heats to decrease little, not exceeding 2 kcal·mol^{-1}. The energy aspects and geometries of these complexes derived from group A are close to those of group A complexes, the monohydration case, except for the geometries of the complex BR in which there is only one hydrogen bond between the HNO and the water molecule that directly link with the HNO molecule in the complex BR, and it is greatly different from the geometries of the reactants of the other groups.

Mechanisms considering dihydration, trihydration, and tetrahydration in loop are also characterized. The reaction energies are 30.5, 28.9, and 28.9 kcal·mol^{-1}, respectively, for the further hydrations from the dihydration to the tetrahydration, being by about 5.0, 6.6, and 6.6 kcal·mol^{-1} lower than the monohydration pathway. The corresponding activation energy lowerings are 41.7, 43.5, and 41.8 kcal·mol^{-1} for the forward ones and 30.9, 30.9, and 29.4 kcal·mol^{-1} for the backward ones, respectively, compared to the unhydrated case (72.6 and 31.3 kcal·mol^{-1}). Analysis regarding the geometries and energy aspects reveals that the effect of waters in the later three hydration assisting pathways on the isomerizations is at the same level and there is no obvious effect on the energies of the reactions when the number of water molecules is larger than four. The effect of the out-of-loop water molecules is also explained with the premise of not more than four water molecules in the complexes. A similar phenomenon has been observed for the surrounding effect arising from other waters around the reaction loop, viz. that increasing out-of-loop water molecules does not significantly change these energy quantities for each of the hydration cases.

The comparison of the four different pathways is also elaborated, including the geometries and energetics. Most of the angles of the two complexes LR and LP reach their optimal values, so it can be considered that the geometries of the complexes LR and LP are more optimal than those of all other complexes. The forward barrier, the backward barrier, and the reaction heat of group L are the lowest among four water-assisting isomerization mechanisms. So we can conclude that the trihydration in-loop assisting isomerization is the best for proton transfer between the atoms N and O in the HNO/HON molecular system. It also can be considered that three water molecules is the best number for the intramolecular proton transfer in the HNO/HON system via forming a molecular loop. The most optimal energy quantities for the water-assisting interconversion (HNO → HON) on the singlet state PES are 29.1 kcal·mol^{-1} for the forward activation energy, 0.21 kcal·mol^{-1} for the backward activation energy, and 28.9 kcal·mol^{-1} for the reaction heat, respectively, at the B3PW91/6-311++G** level. Actually, such a hydration assisting isomerization pathway may exist in the water-dominated environments, for example, in the organism, and thus is of interest to the energy transferring and the NO/HNO-related metabolism processes. Certainly, further studies regarding many other aspects of these systems, such as water-assisting HNO/HON isomerizations in the triplet state, the water effect on the triplet−singlet state energy differences of HNO and HON, and the water effect on the relative preference of the isomerizations with respect to the dissociation channels, etc., are still needed.

Acknowledgment. This work is supported by the National Natural Science Foundation of China (20273040) and the Natural Science Foundation of Shandong Province (Key project). Support from SRFDP is also acknowledged.

Supporting Information Available: Figures, the corresponding Cartesian coordinates, and some values of dihedral angles for the structures of all complexes and transition states calculated at B3PW91/6-311++G** level of the complexes. This material is available free of charge via the Internet at http://pubs.acs.org.

References and Notes

(1) Kerwin, J. F., Jr.; Lancaster, J. R.; Feldman, P. L. *J. Med. Chem.* **1995**, *38*, 4342.

(2) Fukuto, J. M.; Cho, J. Y.; Switzer, C. H. In *Nitric Oxide Biology and Pathobiology*; Ignarro, L. J., Ed.; Academic: San Diego, CA, 2000; pp 23−40.

(3) Grätzel, M.; Taniguchi, S.; Henglein, A. *Ber. Bunsen-Ges. Phys. Chem.* **1970**, *74*, 1003.

(4) Bazylinski, D. A.; Hollocher, T. C. *Inorg. Chem.* **1985**, *24*, 4285.

(5) Fukuto, J. M.; Stuehr, D. J.; Feldman, P. L.; Bova, M. P.; Wong, P. *J. Med. Chem.* **1993**, *36*, 2666.

(6) Wong, P. S.-Y.; Hyun, J.; Fukuto, J. M.; Shirota, F. N.; DeMaster, E. G.; Shoman, D. W.; Nagasawa, H. T. *Biochemistry* **1998**, *37*, 5362.

(7) Murphy, M. E.; Sies, H. *Proc. Natl. Acad. Sci. U.S.A.* **1991**, *88*, 10860.

(8) Bahr, N.; Guller, R.; Reymond, J.-L.; Lerner, R. A. *J. Am. Chem. Soc.* **1996**, *118*, 3550.

(9) Wink, D. A.; Feelisch, M.; Fukuto, J.; Chistodoulou, D.; Jourd'heuil, D.; Grisham, M. B.; Vodovotz, Y.; Cook, J. A.; Krishna, M.; DeGraff, W. G., et al. *Arch. Biochem. Biophys.* **1998**, *351*, 66.

(10) Fukuto, J. M.; Chiang, K.; Hszieh, R.; Wong, P.; Chaudhuri, G. *J. Pharmacol. Exp. Ther.* **1992**, *263*, 546.

(11) Maier, G.; Reisenauer, H. P.; Marco, M. D. *Angew. Chem., Int. Ed.* **1999**, *38*, 108.

(12) Bartberger, M. D.; Fukuto, J. M.; Houk, K. N. *PNAS* **2001**, *98*, 2194.

(13) Liochev, S. I.; Fridovich, I. *Free Radical Biol. Med.* **2003**, *34*, 1399.

(14) Miranda, K. M.; Paolocci, N.; Katori, T.; Thomas, D. D.; Ford, E.; Bartberger, M. D.; Espey, M. G.; Kass, D. A.; Feelisch, M.; Fukuto, J. M.; Wink, D. A. *Proc. Natl. Acad. Sci. U.S.A.* **2003**, *100*, 9196.

(15) Cook, N. M.; Shinyashiki, M.; Jackson, M. I.; Leal, F. A.; Fukuto, J. M. *Arch. Biochem. Biophys.* **2003**, *410*, 89.

(16) Ivanova, J.; Salama, G.; Clancy, R. M.; Schor, N. F.; Nylander, K. D.; Stoyanovsky, D. A. *J. Biol. Chem.* **2003**, *278*, 42761.

(17) Ohshima, H.; Tatemichi, M.; Sawa, T. *Arch. Biochem. Biophys.* **2003**, *417*, 3.

(18) Kaur, H.; Hughes, M. N.; Green, C. J.; Naughton, P.; Foresti, R.; Motterlini, R. *FEBS Lett.* **2003**, *543*, 113.

(19) Naughton, P.; Foresti, R.; Bains, S. K.; Hoque, M.; Green, C. J.; Motterlini, R. *J. Biol. Chem.* **2002**, *277*, 40666.

(20) Culotta, E.; Koshland, D. E., Jr. *Science* **1992**, *258*, 1861.

(21) Stamler, J. S.; Singel, D. J.; Loscalzo, J. *Science* **1992**, *258*, 1898.

(22) Snyder, H. *Nature* **1994**, *372*, 504.

(23) Feelish, M.; te Poel, M.; Zamoora, R.; Deussen, A.; Moncado, S. *Nature* **1994**, *368*, 62.

(24) Miller, J. A.; Bowman, C. T. *Prog. Energy Combust. Sci.* **1989**, *15*, 287.

(25) Alexander, M. H.; Dagdigian, P. J.; Jacox, M. E.; Colb, C. E.; Melius, C. F.; Rabits, J.; Smooke, M. D.; Tsang, W. *Prog. Energy Combust. Sci.* **1991**, *17*, 263.

(26) Sicilia, E.; Russo, N.; Mineva, T. *J. Phys. Chem.* **2001**, *105*, 442−450

(27) Jalbout, A. F.; Darwish, A. M.; Alkahby, H. Y. *J. Mol. Struct.* (*THEOCHEM*) **2002**, *585*, 199−203

(28) Jalbout,A. F. *Chem. Phys. Lett.* **2001**, *340*, 571.

(29) Lee, T. J.; Dateo, C. E. *J. Chem. Phys.* **1995**, *103*, 9110.

(30) Alikhani, M. E.; Dateo, C. E.; Lee, T. J. *J. Chem. Phys.* **1997**, *107*, 8208.

(31) Peters, N. J. S. *J. Phys. Chem. A* **1998**, *102*, 7001.

(32) Kar, T.; Scheiner, S.; Sannigrahi, A. B. *J. Phys. Chem. A* **1998**, *102*, 5967.

(33) Mordaunt, D. H.; Flothmann H.; Stumpf, M.; Keller, H.-M.; Beck, C.; Schinke, R.; Yamashita, K. *J. Chem. Phys.* **1997**, *107*, 6603 and references therein.

(34) Dalby, F. W. *Can J. Chem.* **1958**, *36*, 1336.

(35) Bruma, P. J.; Marian, C. M. *Chem. Phys. Lett.* **1979**, *67*, 109.

(36) Bruma, P. J. *Chem. Phys.* **1980**, *49*, 39.

(37) Heiberg, A.; Almlof, J. *Chem. Phys. Lett.* **1982**, *85*, 542.

(38) Walch, S. P.; Rohlfing, C. M. *J. Chem. Phys.* **1989**, *91*, 2939.

(39) Guadagnini, R.; Schatz, G. C.; Walch, S. P. *J. Chem. Phys.* **1995**, *102*, 774.

(40) Bu, Y. *Chem. Phys. Lett.* **2002**, *338*, 181.

(41) Bu, Y. *Chem. Phys.* **2001**, *273*, 103.

(42) Bu, Y.; Han, K. *J. Phys. Chem. A* **2002**, *106*, 11897.

(43) Frisch, M. J.; Trucks, G. W.; Schlegel, H. B.; Scuseria, G. E.; Robb, M. A.; Cheeseman, J. R.; Zakrzewski, V. G.; Montgomery, J. A., Jr.; Stratmann, R. E.; Burant, J. C.; Dapprich, S.; Millam, J. M.; Daniels, A. D.; Kudin, K. N.; Strain, M. C.; Farkas, O.; Tomasi, J.; Barone, V.; Cossi, M.; Cammi, R.; Mennucci, B.; Pomelli, C.; Adamo, C.; Clifford, S.; Ochterski, J.; Petersson, G. A.; Ayala, P. Y.; Cui, Q.; Morokuma, K.; Malick, D. K.; Rabuck, A. D.; Raghavachari, K.; Foresman, J. B.; Cioslowski, J.; Ortiz, J. V.; Stefanov, B. B.; Liu, G.; Liashenko, A.; Piskorz, P.; Komaromi, I.; Gomperts, R.; Martin, R. L.; Fox, D. J.; Keith, T.; Al-Laham, M. A.; Peng, C. Y.; Nanayakkara, A.; Gonzalez, C.; Challacombe, M.; Gill, P. M. W.; Johnson, B.; Chen, W.; Wong, M. W.; Andres, J. L.; Gonzalez, C.; Head-Gordon, M.; Replogle, E. S.; Pople, J. A. *Gaussian 98*, Revision A.9; Gaussian, Inc.; Pittsburgh, PA, 1998.

(44) Becke, A. D. *J. Chem. Phys.* **1993**, *98*, 5648.

(45) Lee, C.; Yang, W.; Parr, R. G. *Phys. Rev. B* **1998**, *37*, 785.

(46) Vosko, S. H.; Wilk, L.; Nusair, M. *Can. J. Phys.* **1980**, *58*, 1200.

(47) Perdew, J. P. *Phys. Rev. B* **1986**, *33*, 8822.

(48) Perdew, J. P. *Phys. Rev. B* **1986**, *34*, 7406.

(49) Perdew, J. P.; Chevary, J. A.; Vosko, S. H.; Jackson, K, A.; Pederson, M. R.; Singh, D. J.; Fiolhais, C. *Phys. Rev. B* **1992**, *46*, 6671.

(50) Linstrom, P. J.; Mallard, W. G., Eds. *NIST Chemistry WebBook*, NIST Standard Reference Database No. 69; National Insitute of Standards and Technology: Gaithersburg MD, 2001; p 20899 (http://webbook.nist.gov).

(51) Travers, M. J.; Cowles, D. C.; Ellison, G. B. *Chem. Phys. Lett.* **1989**, *164*, 449.